Modeling and Dynamic Exploration of a Tilt-Rotor VTOL Aircraft

Giuseppe Notarstefano * **John Hauser** **

* *Department of Engineering, University of Lecce, Via per Monteroni, 73100, Lecce, Italy (e-mail: giuseppe.notarstefano@unile.it)*
** *Department of Electrical and Computer Engineering, University of Colorado, Boulder, USA (e-mail: hauser@colorado.edu)*

Abstract: In this paper we introduce and study a novel model of a Tilt-Rotor VTOL aircraft. The aircraft is structured as a blended wing body equipped with a tilting rotor (the propulsion unit) that gives the vehicle the capability of vertical take off and transition to a forward flight configuration. This model captures the main features of novel tilt-rotor aircraft architectures with more challenging control and maneuvering capabilities. We introduce a complex nine degrees of freedom model of the aircraft to explore the dynamics and the maneuvering capabilities of the vehicle. We perform an analysis of the equilibrium manifold of the aircraft (namely a parametrized family of trimming trajectories) and, as main contribution of the paper, we introduce a set of optimal control based strategies to explore the trajectory manifold of the vehicle in order to generate non-stationary and highly aggressive trajectories. In particular, we provide numerical computations showing how to generate a trajectory for transitions from near hover to forward flight.

Keywords: VTOL aircraft, tilt-rotor, aggressive maneuvering, optimal control

1. INTRODUCTION

A new interesting frontier in the design of aerial vehicles is the development of aircrafts with novel configurations that allow for a richer set of maneuvering capabilities. In 1934 a US patent was granted to Blount for his "airplane-helicopter". Since then many attempts have been done in the last century to design novel architectures based on a tilt-rotor(s) configuration. The twin tilt-rotor V22-Osprey is certainly one of the most famous aircrafts in this class for being both the first one approved for full-scale development but also the one being grounded after two crashes in 2000. The presence of two rotors was one of the causes of unreliability of such configuration. Recently, novel architectures have been proposed with a unique tilting rotor suitably placed in the fixed wing structure, see, e.g., patents Pham (2005), Mioduchevski (2008a) and Burrage (2009). The tilt-rotor aircraft model that we introduce in the paper is based on a new prototype of UAV (Uninhabited Aerial Vehicle) proposed in patents Mioduchevski (2008a) and Mioduchevski (2008b). The control literature on tilt-rotor aircrafts is almost absent. At the best of our knowledge the only references are Calise and Rysdyk (1998) and Kendoul et al. (2006), where respectively a neural network and a backstepping based control law were proposed for a twin tilt-rotor architecture. A wider literature can be found on vertical take off and landing aircrafts with capabilities of transition to forward flight. The well known flying wing Caltech Ducted Fun, developed at Caltech, was introduced in Jadbabaie et al. (1999) and control strategies for transition maneuvers from hover to forward flight were studied in later works, see, e.g., Jadbabaie and Hauser (2002). More recently a novel architecture of UAV (Uninhabited Aerial Vehicle) was introduced in Marconi and Naldi (2006). The UAV consists of a rigid structure holding a ducted fan and a set of active flaps providing full control to the vehicle and capability of transition to forward flight.

In this paper we aim at investigating the maneuvering capabilities of tilt-rotor aircrafts. The main challenge is to model and explore different dynamic and aerodynamic regimes. In particular, we aim at understanding how to design trajectories that involve a transition from hover to forward flight configurations. The main contributions of the paper are three. First, we introduce a novel model of a Tilt-Rotor VTOL aircraft suitable for optimization and control. We call this model TR-VTOL. In particular, we provide a full nine degrees of freedom dynamic model with four rigid bodies (a blended wing body, a tilting gimbal, a yaw gimbal and a propeller), aerodynamics and thurst model. Second, we characterize the equilibrium manifold of the TR-VTOL aircraft. That is, we study stationary (trimming) trajectories of the vehicle and parametrize them with respect to suitable parameters, i.e., the vehicle speed, the flight path angle and the orientations of the tilting rotor. Third, we explore the dynamic capabilities of the vehicle by use of optimal control tools. We provide a strategy to compute non-stationary trajectories of the TR-VTOL, based on the Projection Operator Newton

⋆ The authors would like to thank Prof. Pavel Mioduchevski of I.A.S. s.r.l. for developing such an exciting aircraft and for helpful discussions on modeling. We thank I.A.S. s.r.l. for establishing a fruitful research collaboration, including support for a visit by the second author at the University of Lecce. This research was supported in part by the US AFOSR under grant FA9550-09-1-0470.

method for optimization of trajectory functionals, Hauser (2002). To show the effectiveness of this tool we present a trajectory for performing a transition maneuver from a near hovering to forward flight configuration.

2. TILT-ROTOR VTOL AIRCRAFT MODEL

In this section we introduce the novel tilt-rotor aircraft model, the TR-VTOL, studied in the paper. We develop a complex nine degrees of freedom model using a Lagrangian approach. The TR-VTOL model is based on the aircraft prototype proposed in the patents Mioduchevski (2008a) and Mioduchevski (2008b) depicted in Figure 1. It consists of a blended wing body and an orientable propulsion unit. The propulsion unit, located in the blended wing, consists of a propeller and two moving gimbals to rotate the propeller about the two axes in the horizontal plane of the blended wing.

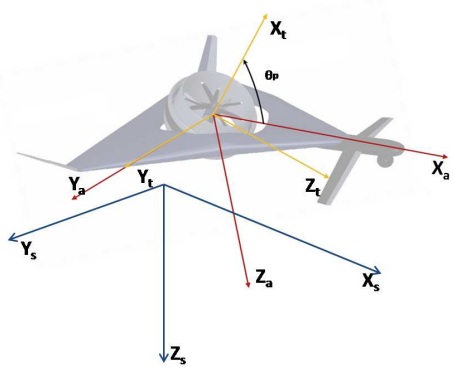

Fig. 1. The tilt-rotor VTOL aircraft prototype proposed in Mioduchevski (2008a) together with examples of the reference frames introduced in Section 2.1. Specifically: spatial frame F_s (blue), aircraft frame F_a (red) and tilt frame F_t (yellow).

2.1 Reference frames and generalized coordinates

We model the tilt-rotor VTOL aircraft as a four-rigid-body system driven by aerodynamic forces and moments generated by the structure, a thrust force generated by the propeller and internal torques between the rigid components to rotate the propulsion gimbals. The four rigid bodies are: the main aircraft body, the propulsion tilt (or pitch) gimbal, the propulsion yaw gimbal, and the rotating propeller with the shaft. Consistently with the four-rigid-body structure, we introduce four reference frames attached to the bodies

- F_a - **aircraft** frame (airframe) [1]
- F_t - propulsion **tilt** (or pitch) frame
- F_r - propulsion yaw (or **rudder**) frame
- F_p - **propeller** frame.

We assume that all four reference frames have the same origin being the point of intersection of the three gimbal planes.

Before introducing the configuration variables we need some notation. Given a rigid body with frame F_b attached to the body, we let $x \in \mathbb{R}^3$ and $R \in SO(3)$ denote the position and orientation of the frame F_b (fixed at a point of the body) with respect to a fixed inertial (or spatial) frame F_s with x-y-z axes oriented in a north-east-down (or, locally, forward-right-down) fashion. R maps vectors in the body frame to vectors in the spatial frame so that, for instance, the spatial angular velocity ω and the body angular velocity ω_b are related by $\omega = R\omega_b$ and $\omega_b = R^T\omega$. Here the adjectives spatial and body refer to the frame (or basis) in which the vector is expressed. Similarly, $p = x + Rp_b$ gives the spatial coordinates of a point on the body with body coordinates $p_b \in \mathbb{R}^3$. Abusing notation, we will sometimes write $x = (x, y, z)^T$ with context indicating whether x is the position vector or the scalar first component of the position vector. It is often useful to parametrize the rotation R in terms of *principal axis* rotations, i.e., (simple) rotations about one of the axes, in the "moving" frame. To do that, we let $R_x(\varphi)$, $R_y(\theta)$ and $R_z(\psi)$ be respectively a rotation of an angle φ about the x axis, of θ about the y axis and of ψ about the z axis so that, for example,

$$R_x(\varphi) = \begin{bmatrix} 1 & 0 & 0 \\ 0 & c_\varphi & -s_\varphi \\ 0 & s_\varphi & c_\varphi \end{bmatrix},$$

where we use notation c_φ for $\cos\varphi$ and s_φ for $\sin\varphi$. A widely used parametrization for the rotation matrix R is the Roll-Pitch-Yaw, $R = R_z(\psi)\, R_y(\theta)\, R_x(\varphi)$, where φ, θ and ψ are respectively the roll, pitch and yaw angles and the order of the rotations expresses the fact that the yaw rotation comes first followed by pitch and roll. The mapping $(\varphi, \theta, \psi) \mapsto R$ is locally one-to-one and onto (i.e., there are no singularities) in the region $|\theta| < \pi/2$, $|\varphi| < \pi/2$.With this in hand we can define the generalized coordinates for the model. We let $x = (x, y, z)$ be the spatial position of the aircraft frame F_a (and all other frames). The roll, pitch and yaw angles φ, θ, ψ parametrize the orientation of the airframe (the aircraft frame). The orientation of the propulsion unit is parametrized by the propulsion pitch angle (the angle of the pitch gimbal) θ_p, the propulsion yaw angle (the angle of the yaw/rudder gimbal) ψ_p and the propeller shaft angle φ_p ($\dot{\varphi}_p$ is the propeller rotation speed). The angle θ_p is defined so that $\theta_p \approx 0$ in forward flight and $\theta_p \approx \frac{\pi}{2}$ in hover. In Figure 1 we show the spatial, aircraft and tilt frames. In particular, we highlight the angle θ_p between the tilt frame and the aircraft frame. For sake of compactness we introduce the notation $\phi = (\varphi, \theta, \psi)^T$, $\phi_p = (\varphi_p, \theta_p, \psi_p)^T$ and $\xi = (\phi^T, \phi_p^T)^T$. We underline the difference between the two versions of the Greek letter *phi*, i.e., scalar φ and vector ϕ. We restrict the range of operation of the aircraft to the operating region $\{(x, \phi, \phi_p) \in \mathbb{R}^9 \mid |\varphi| < \pi/2, |\theta| < \pi/2, -\frac{\pi}{4} < \theta_p < \frac{3\pi}{4}, |\psi_p| < \frac{\pi}{4}\}$ [2]. On this operating region the vector

$$q = (x, y, z, \varphi, \theta, \psi, \varphi_p, \theta_p, \psi_p) = (x, \phi, \phi_p) = (x, \xi)$$

provides a valid set of generalized coordinates for dynamics calculations. We can thus express the orientation of each reference frame in terms of the angular generalized coordinates. The orientation R_p of the propeller frame is, for example,

[1] This frame is attached to the blended wing body, but, in fact, it defines the configuration of the whole aircraft. Thus the notation aircraft frame.

[2] Having limited ϕ, θ, θ_p and ψ_p, we can take every angle belonging to $\mathbb{R}$ instead of S^1

$$R_p(\phi,\phi_p) = R_z(\psi)\,R_y(\theta)\,R_x(\varphi)\,R_y(\theta_p)\,R_z(\psi_p)\,R_x(\varphi_p).$$

The order of the rotations expresses the fact that rotation of the airframe is described by a roll, pitch and yaw convention where the yaw rotation is the first, followed by the pitch and roll ones. For the propulsion unit, the propulsion pitch rotation comes first followed by the propulsion yaw and the propeller shaft angle rotations. The rotations of the intermediate frames are obtained by setting to zero the angles corresponding to the subsequent frames, so that, for example, the rotation R_a for the airframe F_a is given by $R_a(\phi) = R_z(\psi)\,R_y(\theta)\,R_x(\varphi)$. Vectors are given a subscript representing the rigid body they refer to and a superscript representing the frame they are expressed into. Vectors expressed in the corresponding body frame are not given any superscript. Thus, for instance, the angular velocity of the propeller satisfies

$$\begin{aligned}\omega_p^s &= R_a(\phi)\,\omega_p^a = R_a(\phi)R_y(\theta_p)\,\omega_p^t = R_t(\phi,\theta_p)\,\omega_p^t \\ &= R_a(\phi)R_y(\theta_p)R_z(\psi_p)R_x(\varphi_p)\,\omega_p = R_p(\phi,\phi_p)\,\omega_p.\end{aligned}$$

2.2 Kinetic and potential energy

We develop the kinetic and potential energy terms to compute the system dynamics. For a multi-body system the kinetic (potential) energy is the sum of the kinetic (potential) energies of each rigid body. Thus, for our model the kinetic energy is

$$T = T_a + T_t + T_r + T_p.$$

The kinetic energy of a general rigid body with corresponding reference frame F_ν is the sum of the translational and rotational kinetic energies

$$T_\nu = T_\nu(\phi,\phi_p,\dot{x},\dot{\phi},\dot{\phi}_p) = \frac{1}{2}m_\nu\|v_\nu^s\|^2 + \frac{1}{2}\omega_\nu^T\mathbb{I}_\nu\omega_\nu,$$

where v_ν^s is the linear velocity vector of the center of mass (of the rigid body) expressed in the spatial frame F_s, ω_ν is the angular velocity vector expressed in the reference frame F_ν, m_ν is the mass of the rigid body and $\mathbb{I}_\nu$ the inertia tensor (about the center of mass). We can write the kinetic energy in terms of the generalized coordinates and velocities (q and $\dot{q}$) as

$$T_\nu = T_\nu(\phi,\phi_p,\dot{x},\dot{\phi},\dot{\phi}_p) = T_\nu(\xi,\dot{x},\dot{\xi}) = \frac{1}{2}\dot{q}^T M_\nu(q)\,\dot{q},$$

where $M_\nu(q)$ is the mass matrix associated to F_ν. The mass matrix turns to be

$$\begin{aligned}M_\nu(q) &= M_\nu(\xi) \\ &= \begin{bmatrix} m_\nu I & -m_\nu R_\nu(\xi)\,\widehat{x}_{\nu c}J_{\omega_\nu}(\xi) \\ -m_\nu J_{\omega_\nu}(\xi)^T\widehat{x}_{\nu c}^T R_\nu(\xi)^T & J_{\omega_\nu}(\xi)^T\mathbb{I}_{\nu o}J_{\omega_\nu}(\xi)\end{bmatrix}\end{aligned}$$

where $\widehat{x}_{\nu c}$ is the (skew-symmetric) matrix representation of the linear mapping $v \mapsto x_{\nu c}\times v = \widehat{x}_{\nu c}v$, $J_{\omega_\nu}(\xi)$ is the *Jacobian* mapping to express the angular velocity of the rigid body F_ν in terms of the generalized velocities ($\omega_\nu = J_{\omega_\nu}(\xi)\,\dot{\xi}$) and $\mathbb{I}_{\nu o} = \mathbb{I}_\nu + m_\nu\widehat{x}_{\nu c}^T\widehat{x}_{\nu c}$.

The potential energy is given by

$$V = V_a + V_t + V_r + V_p.$$

The general contribution for the reference frame F_ν is

$$V_\nu = V_\nu(\phi,\phi_p) = V_\nu(\xi) = -m_\nu g\,e_3^T x_\nu^s$$

where x_ν^s is the spatial position of the center of mass of the rigid body corresponding to F_ν.

2.3 Aerodynamic and propulsion forces and torques

The forces and moments acting on the system are given by: (i) aerodynamics, acting on both the wing body and the propulsion system, (ii) thrust force generated by the propeller, and (iv) internal torques to orient the propulsion gimbal. The aerodynamic forces and moments are obtained by using a classical formulation in flight dynamics. To this end, given a wing profile whose frame is F_ν, let F_w denote the classical wind frame, i.e., a reference frame whose x-axis points in the direction of the velocity vector, and the y and z axes are chosen so that vectors in the wind frame are transformed into the body frame with two simple rotations R_y(-α) and $R_z(\beta)$. The angles α and β are called *angle of attack* and *side-slip angle* respectively, and are defined as

$$\tan\alpha = v_{\nu 3}/v_{\nu 1} \qquad \text{and} \qquad \beta = \arcsin(v_{\nu 2}),$$

where $v_\nu = (v_{\nu 1}, v_{\nu 2}, v_{\nu 3})^T$ is the velocity of the point of application of the aerodynamic forces expressed in the body frame F_ν. The rotation matrix $R_{bw}(\alpha,\beta)$ transforming vectors from the wind frame into the body frame is given by

$$R_{bw}(\alpha,\beta) = R_y(\text{-}\alpha)R_z(\beta) = \begin{bmatrix} c_\alpha c_\beta & -c_\alpha s_\beta & -s_\alpha \\ s_\beta & c_\beta & 0 \\ s_\alpha c_\beta & -s_\alpha s_\beta & c_\alpha \end{bmatrix}.$$

The aerodynamic forces, acting in the wind frame, are the drag force $\mathbf{D}_\nu$, the side force $\mathbf{Y}_\nu$ and the lift force $\mathbf{L}_\nu$. They are expressed in terms of dimensionless coefficients depending on the angle of attack and sideslip angle, the angular velocity vector ω_ν and the deflections (in radians) of active control surfaces $\delta_{a\nu}$ (aileron), $\delta_{e\nu}$ (elevator) and $\delta_{r\nu}$ (rudder),

$$\begin{aligned}\begin{bmatrix}\mathbf{D}_\nu \\ \mathbf{Y}_\nu \\ \mathbf{L}_\nu\end{bmatrix} &= \tfrac{1}{2}\rho S_\nu\|v_\nu^s\|^2\big[C_{0\nu}^F(\alpha,\beta) + C_{\omega\nu}^F(\alpha,\beta)\omega \\ &\quad + C_{\delta_a\nu}^F(\alpha,\beta)\delta_{a\nu} + C_{\delta_e\nu}^F(\alpha,\beta)\delta_{e\nu} + C_{\delta_r\nu}^F(\alpha,\beta)\delta_{r\nu}\big],\end{aligned}$$

where S_ν is the wing profile surface, v_ν^s is the velocity of the aerodynamic center (point of application of aerodynamic forces and moments) expressed in the spatial frame and $C_{0\nu}^F,\ldots,C_{\delta_r\nu}^F \in \mathbb{R}^3$ are dimensionless coefficient vectors. We consider only the contribution of the aerodynamics acting on the wing body and neglect the contribution on the propulsion unit. The aerodynamic forces expressed in the body frame F_a are

$$\mathbf{F}_a = R_{bw}(\alpha,\beta)\begin{bmatrix}\mathbf{D}_a(\alpha,\beta,\omega,\delta_a,\delta_e,\delta_r) \\ \mathbf{Y}_a(\alpha,\beta,\omega,\delta_a,\delta_e,\delta_r) \\ \mathbf{L}_a(\alpha,\beta,\omega,\delta_a,\delta_e,\delta_r)\end{bmatrix},$$

where δ_a, δ_e and δ_r are the deflections (in radians) of the active control surfaces of the aircraft (blended wing) body. The aerodynamic moments are expressed directly in the body frame F_a and are written in terms of dimensionless coefficients as follows

$$\begin{aligned}\mathbf{M}_a = &\tfrac{1}{2}\rho S_a\|v_a^s\|^2\begin{bmatrix}b_a & 0 & 0 \\ 0 & c_a & 0 \\ 0 & 0 & b_a\end{bmatrix}\big[C_0^M(\alpha,\beta) + C_\omega^M(\alpha,\beta)\,\omega \\ &+ C_{\delta_a}^M(\alpha,\beta)\,\delta_a + C_{\delta_e}^M(\alpha,\beta)\,\delta_e + C_{\delta_r}^M(\alpha,\beta)\,\delta_r\big],\end{aligned}$$

where S_a, b_a and c_a are respectively the surface, the span and the chord of the aircraft (blended wing) body and $C_0^M,\ldots,C_{\delta_r}^M \in \mathbb{R}^3$ are dimensionless coefficient vectors. Using classical disc actuator theory, see, e.g., Stengel (2004), it is possible to obtain an expression of the thrust

in terms of the propeller velocity. In the paper we consider a simplified thrust model, i.e., we assume that the thrust is entirely directed along the x-axis of F_p (or equivalently F_r) and that we can control directly its amplitude. That is, the thrust is given by $e_1\delta_T$ where δ_T is a control input. Consequently we will neglect the torque generating the propeller rotation. A full characterization of the thrust model is subject of current research and will be of key importance in the exploration of complete transitions from hover to forward flight.

The control inputs vector to maneuver the TR-VTOL is, therefore,

$$u = [\delta_T, \delta_a, \delta_e, \delta_r, \tau_{\theta_p}, \tau_{\psi_p}]^T,$$

where τ_{θ_p} and τ_{ψ_p} are the torques to orient the propulsion directly applied to the generalized velocities $\dot{\theta}_p$ and $\dot{\psi}_p$.

2.4 Lagrangian dynamics

We now determine the dynamics of the system via the Euler-Lagrange equations. To this end, we form the Lagrangian L as the difference between the kinetic and potential energies $L(q, \dot{q}) = T(q, \dot{q}) - V(q)$. The equations of motion are then determined by Euler-Lagrange equations

$$\frac{d}{dt}\frac{\partial L}{\partial \dot{q}}^T - \frac{\partial L}{\partial q}^T = \tau$$

where τ is the set of generalized forces. The generalized forces include, directly, the torques required for orienting the propulsion system as well as, through more complicated Jacobian expressions, the forces and moments arising from aerodynamics and propulsion. Making use of the structure of T and V, we see that the equations of motion have the form

$$M(q)\,\ddot{q} + C(q, \dot{q}) + G(q) = \tau$$

where $M(q)$ is the generalized mass matrix computed in the previous paragraph, $C(q, \dot{q})$ is a vector of generalized forces due to Coriolis and centrifugal effects and that is quadratic in the velocities $\dot{q}$, and $G(q)$ is a vector of generalized forces arising from the potential energy, here due to gravity acting on the body centers of gravity. Since the total energy is given by summing over the energies of each moving body, each of the terms M, C, and G is in fact a sum of the corresponding terms from each body.

Next, we compute the vector of generalized forces τ. We rewrite it as

$$\tau = \tau_{\mathrm{a}} + \tau_{\mathrm{prop}} + \tau_{\mathrm{tilt}}$$

where τ_{a} is the generalized force resulting from the aerodynamic forces and moments acting on the wing body, τ_{prop} is related to the propulsion force and moments, and τ_{tilt} are directly the (generalized) torques to orient the propulsion system. The generalized force τ_a resulting from the aerodynamic forces and moments is obtained as follows. The translational portion, $\tau_{a(1:3)}$, is given by the aerodynamic force transformed to the inertial frame using R_a. The rotational portion, $\tau_{a(4:6)}$, is obtained by transforming the aerodynamic moment using $J_{\omega_a}(\phi)^T$ to obtain a vector of generalized forces conjugate to $\dot{\phi}$. Therefore we have

$$\tau_{\mathrm{a}}(\delta_e, \delta_a, \delta_r) = \begin{bmatrix} R_a \mathbf{F}_a(\delta_e, \delta_a, \delta_r) \\ J_{\omega_a}(\phi)^T \mathbf{M}_a(\delta_e, \delta_a, \delta_r) \\ 0 \end{bmatrix}.$$

The propulsion force and moments are applied in the rudder frame F_r. The propulsion force acts in the direction $R_r\, e_1$. The propulsion moments are transformed to a generalized force using $J_{\omega_r}(\phi, \phi_p)^T$. Therefore we have

$$\tau_{\mathrm{prop}}(\delta_T) = \begin{bmatrix} R_r\, e_1 \delta_T \\ 0 \end{bmatrix}.$$

The torques τ_{θ_p} and τ_{ψ_p} required for orienting the propulsion system are directly applied to the generalized velocities $\dot{\theta}_p$ and $\dot{\psi}_p$. Therefore

$$\tau_{\mathrm{tilt}}(\tau_{\theta_p}, \tau_{\psi_p}) = \begin{bmatrix} 0 & 0 & 0 & 0 & 0 & 0 & \tau_{\theta_p} & \tau_{\psi_p} & 0 \end{bmatrix}^T.$$

3. EQUILIBRIUM MANIFOLD

In this section we analyze the equilibrium manifold of the TR-VTOL, i.e. the set of all flight trajectories for which the dynamically important variables are constant. The key purpose of this study is to develop an understanding of the range of model validity. The resulting set of trajectories is a family of helicoidal trajectories that is symmetric with respect to rotations about a vertical axis. In the flight dynamics literature these "constant trajectories" are often referred to as trimming trajectories and the procedure of computing them is known as "trimming the aircraft". For the TR-VTOL aircraft, we require that the propulsion system configuration (θ_p, ψ_p) be constant. This implies that the system may be treated as a typical aircraft, with the exception that hovering is possible. Finding constant trajectories requires the solution of a set nonlinear equations expressing the fact that all accelerations must be set to zero (except those lateral accelerations providing a constant turn rate). In looking at the equilibrium manifold we assume that the constant trajectories are performed with zero sideslip angle ($\beta = 0$). This way of flying the aircraft is often referred to as "coordinated flight". Under this assumption, we can parametrize the aircraft linear velocity on the helicoidal trajectory by means of the velocity norm $V = \|\dot{x}_a^s\|$, the flight path angle $\gamma = \theta - \alpha$, the yaw angle ψ and the lateral acceleration a_l, as

$$\begin{aligned} \dot{x} &= \;\; V\cos\psi\cos\gamma \\ \dot{y} &= \;\; V\sin\psi\cos\gamma \\ \dot{z} &= -V\sin\gamma \\ \dot{\psi} &= \;\; a_l/(V\cos\gamma). \end{aligned}$$

Due to the symmetry of the system, the dynamics is invariant with respect to translations and yaw rotations. Therefore, without loss of generality we can pose $(x, y, z) = (0, 0, 0)$ and $\psi = 0$ to search for the equilibria. By these arguments, we have the following expression for the equilibrium generalized coordinates, velocities and accelerations

$$\begin{aligned} q_e &= [0\ 0\ 0\ \varphi_e\ \theta_e\ 0\ 0\ \theta_{pe}\ \psi_{pe}] \\ \dot{q}_e &= [V\cos\gamma\ 0\ V\sin\gamma\ 0\ 0\ a_l\ 0\ 0\ 0] \\ \ddot{q}_e &= [0\ a_l\ 0\ 0\ 0\ 0\ 0\ 0\ 0]. \end{aligned}$$

The set of nonlinear equations to solve is, therefore,

$$M(q_e)\ddot{q}_e + C(q_e, \dot{q}_e) + G(q_e) = \tau_e,$$

where V, γ, a_l, θ_p and ψ_p parameterize the equilibrium manifold and φ_e, θ_e and $\tau_e(\delta_{Te}, \delta_{ae}, \delta_{ee}, \delta_{re}, \tau_{\theta_p e}, \tau_{\psi_p e})$ are obtained by solving the nonlinear equations for the given set of parameters.

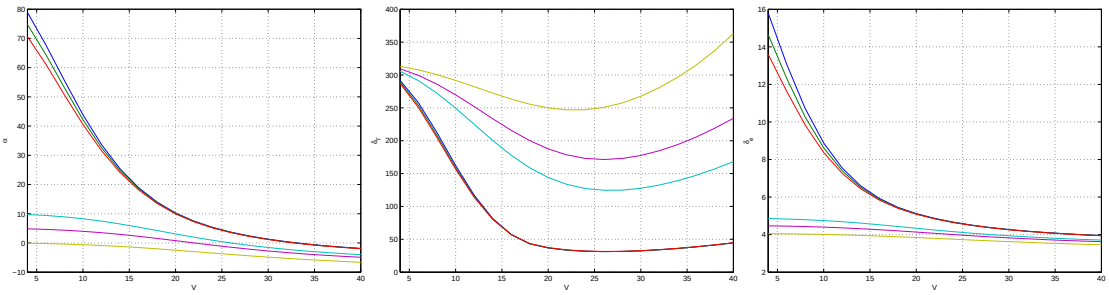

(a) Angle of attack α. (b) Thrust δ_T. (c) Elevator δ_e.

Fig. 2. Equilibrium manifold for constant altitude forward flight. Specifically: V=4-40 m/s, γ=0 deg, a_l=0 m/s^2, θ_p=(0, 5, 10, 80, 85, 90) deg.

We present some slices of the equilibrium manifold for constant altitude forward flight conditions with various propulsion pitch angles. In Figures 2, we depict the set of equilibrium points (constant trajectories) with propulsion angles ranging from those corresponding to forward flight ($\theta_p = 0, 5, 10$ degrees) to those for near hover conditions ($\theta_p = 80, 85, 90$ degrees). Indeed, we can notice that at low speeds (near hover) the only reasonable values for the angle of attack and the elevator are obtained with values of the propulsion angle $\theta_p = 80, 85, 90$ degrees (near hover).

4. TRAJECTORY EXPLORATION

Complex dynamic interactions make the development of maneuvers highly nontrivial. To this end, we use nonlinear least squares trajectory optimization to explore system trajectories. That is, we consider the optimal control problem

$$\begin{aligned} \min \;& \|(x(\cdot), u(\cdot)) - (x_d(\cdot), u_d(\cdot))\|^2_{L_2}/2 \\ \text{subj} \;& \dot{x} = f(x, u)\,, \quad x(0) = x_0\,, \end{aligned}$$

where $\|\cdot\|_{L_2}$ is a weighted L_2 norm on $[0, T]$ [3] and $(x_d(\cdot), u_d(\cdot))$ is a desired curve used as a trajectory exploration design *parameter*. Writing the least squares trajectory functional as $h(\xi) = \|(x(\cdot), u(\cdot)) - (x_d(\cdot), u_d(\cdot))\|^2_{L_2}/2$ with $\xi = (x(\cdot), u(\cdot))$, the optimization problem becomes

$$\min_{\xi \in \mathcal{T}} h(\xi) \tag{1}$$

where $\mathcal{T}$ is the manifold of bounded trajectories $(x(\cdot), u(\cdot))$ on $[0, T]$. To facilitate the local exploration of trajectories of this highly coupled nonlinear system, we use the Projection Operator Newton method developed in Hauser (2002), see also Hauser and Meyer (1998). The time varying trajectory tracking control law

$$\begin{aligned} \dot{x} =& f(x, u), \qquad x(0) = x_0, \\ u(t) =& \mu(t) + K(t)(\alpha(t) - x(t)) \end{aligned}$$

defines the projection operator $\mathcal{P} : \xi = (\alpha, \mu) \mapsto \eta = (x, u)$, taking the curve $\xi = (\alpha, \mu)$ to the trajectory $\eta = (x, u)$. Using the projection operator to locally parametrize the trajectory manifold, we may convert the constrained optimization problem (1) into one of minimizing the unconstrained functional $g(\xi) = h(P(\xi))$. Minimization of the trajectory functional is accomplished by iterating over the following Newton descent method, where ξ_i indicates the current trajectory iterate and ξ_0 is an initial trajectory.

[3] The L_2 weights are design variables that reflect the relative importance (or confidence) of certain components of the desired curve.

Algorithm (projection operator Newton method)
Given initial trajectory $\xi_0 \in \mathcal{T}$
For $i = 0, 1, 2...$

design K defining $\mathcal{P}$ about ξ_i
search direction

$$\zeta_i = \arg \min_{\zeta \in T_{\xi_i}\mathcal{T}} Dg(\xi_i) \cdot \zeta + \frac{1}{2} D^2 g(\xi_i)(\zeta, \zeta)$$

step size $\gamma_i = \arg\min_{\gamma \in (0,1]} g(\xi + \gamma\zeta_i)$;
project $\xi_{i+1} = \mathcal{P}(\xi_i + \gamma_i \zeta_i)$.

end

Note that the two main steps of designing the K and searching for the descent direction involve the solution of suitable (well known) LQ optimal control problems.

Transition maneuver from near hover to forward flight

We present a trajectory for performing a transition maneuver from almost hovering ($V = 5m/s$ and $\theta_p \simeq \pi/2$) to forward flight ($V = 25m/s$ and $\theta_p \simeq 0$) in the longitudinal plane. Although the maneuver lies in the longitudinal plane (with 5 degrees of freedom), it is computed using the complete model with 9 degrees of freedom. In the computation of this transition, a very naive choice was made for the desired trajectory. The two stationary conditions at 5 and $25m/s$ (with corresponding propulsion angles) were computed and then a smooth transition of all configuration variables was chosen. Consequently, generalized velocities which are zero in the trim conditions are taken be zero in the desired trajectory for the entire (varying) transition. Nevertheless, the optimization procedure has no difficulty finding an interesting transition trajectory that satisfies the system dynamics. In effect, the optimization works to *spread out* the inconsistencies in the desired trajectory to obtain a dynamically feasible trajectory. In the process, trade-offs are made that reflect the least squares weighting that has been chosen. The curves in Figure 3 depict the result of the optimization procedure with a choice of L_2 weights for measuring the distance between curves. For this choice, the velocity and altitude follow the desired curves in a reasonable manner. In contrast, the propulsion angle and the thrust exhibit interesting lead and lag phenomena that deserve further attention in the future. Some of the most interesting excursions from the *desired* (and unrealistic) curves are those associated with the aircraft pitch attitude and the elevator input. As noted above, the desired curves were chosen as a smooth combination of two sets of equilibrium values without reflecting what is needed

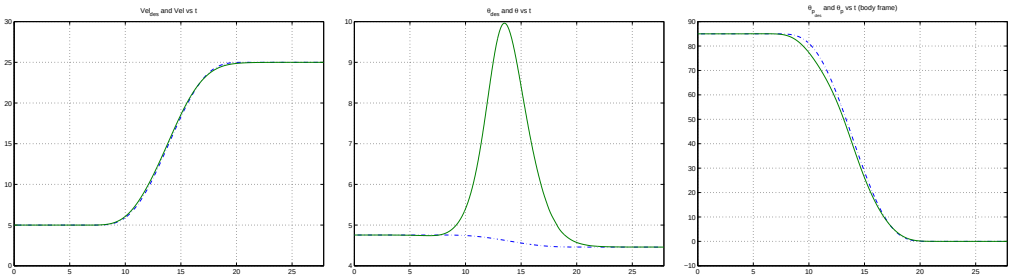

(a) Velocity (V) vs time. (b) Pitch angle (θ) vs time. (c) Prop. pitch angle (θ_p) vs time

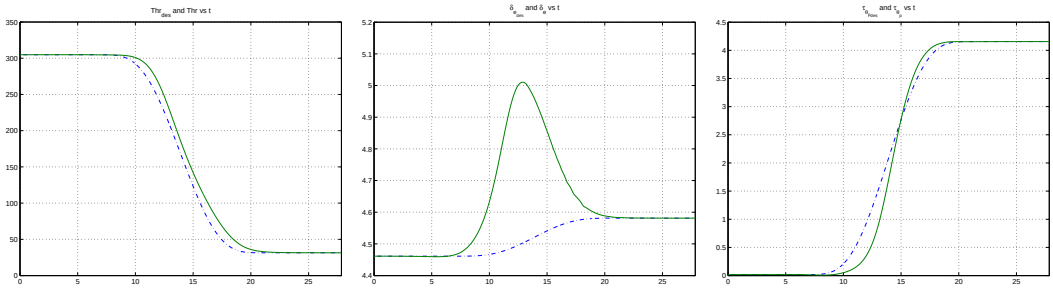

(d) Thrust (δ_T) vs time (e) Elevator (δ_e) vs time (f) Prop. pitch torque (τ_{θ_p}) vs time

Fig. 3. Transition maneuver from quasi hover to forward flight. Specifically: desired transition from $V = 5$m/s to $V = 25$m/s (with propulsion pitch angle varying from $\theta_p = 85$ to $\theta_p = 0$) in 10 seconds at constant altitude. The dashed blue line is the desired curve and the solid green line is the system trajectory.

during maneuvering. To make up for this naive choice of the desired trajectory, the optimization has found that a temporary increase in both pitch and elevator helps in the execution of the transition maneuver. One useful output of the computation is the torque used to orient the propulsion system. Here, we see that, while the torque does not follow the naive desired one, it does stay well within the desired bounds.

5. CONCLUSIONS

In this paper we introduced a novel Tilt-Rotor VTOL aircraft model based on the prototype architecture in Mioduchevski (2008a). The proposed model is still preliminary and allows to study the dynamic capabilities of the aircraft from near hover to forward flight. We characterized the equilibrium manifold of the aircraft model and proposed an optimal control based strategy to explore the dynamic capabilities of the aircraft in highly non-stationary regimes. We provided numerical computations showing an example transition maneuver from near hover to forward flight. Future work includes the development of more accurate propulsion and aerodynamic models to deal with full transitions from hover to forward flight and, consequently, a full dynamic exploration of the system maneuvering capabilities.

REFERENCES

Burrage, R.G. (2009). Tilt-rotor aircraft. Patent US7584923, United States.

Calise, A. and Rysdyk, R.T. (1998). Nonlinear adaptive flight control using neural networks. *IEEE Control Systems Magazine*, 18(6), 14–25.

Hauser, J. (2002). A projection operator approach to the optimization of trajectory functionals. In *IFAC World Congress*. Barcelona.

Hauser, J. and Meyer, D.G. (1998). The trajectory manifold of a nonlinear control system. In *IEEE Conf. on Decision and Control*, volume 1, 1034–1039.

Jadbabaie, A. and Hauser, J. (2002). Control of a thrust-vectored flying wing: a receding horizon - lpv approach. *International Journal of Robust and Nonlinear Control*, 12(9), 869–896.

Jadbabaie, A., Yu, J., and Hauser, J. (1999). Receding horizon control of the caltech ducted fan: a control lyapunov function approach. In *IEEE Int. Conf. on Control Applications*, volume 1, 51–56. Kohala Coast, HI, USA.

Kendoul, F., Fantoni, I., and Lozano, R. (2006). Modeling and control of a small autonomous aircraft having two tilting rotors. *IEEE Transactions on Robotics*, 22(6), 1297–1302.

Marconi, L. and Naldi, R. (2006). Nonlinear robust control of a reduced-complexity ducted mav for trajectory tracking. In *IEEE Conf. on Decision and Control*. San Diego, CA.

Mioduchevski, P. (2008a). Convertible aircraft. Patent EP1999016, Europe, Assignee: International Aviation Supply I.A.S. S.R.L., Brindisi, IT).

Mioduchevski, P. (2008b). Convertible aircraft. Patent, United States, Assignee: International Aviation Supply I.A.S. S.R.L., Brindisi, IT). Pending.

Pham, R.N. (2005). High performance VTOL convertiplanes. Patent US6974105, United States.

Stengel, R. (2004). *Flight Dynamics*. Princeton University Press.